




# Characterizing dominant patterns of spatiotemporal variation for a transboundary groundfish assemblage

Lukas B. DeFilippo<sup>1,2</sup> | James T. Thorson<sup>3</sup> | Cecilia A. O'Leary<sup>1</sup>  |  
Stan Kotwicki<sup>1</sup>  | Jerry Hoff<sup>1</sup> | James N. Ianelli<sup>4</sup> | Vladimir V. Kulik<sup>5</sup>  |  
Andre E. Punt<sup>2</sup>

<sup>1</sup>Resource Assessment and Conservation Engineering Division, Alaska Fisheries Science Center, NOAA, NMFS, Seattle, WA, USA

<sup>2</sup>School of Aquatic and Fishery Science, University of Washington, Seattle, WA, USA

<sup>3</sup>Habitat and Ecological Processes Research Program, Alaska Fisheries Science Center, NOAA, NMFS, Seattle, WA, USA

<sup>4</sup>Resource Ecology and Fisheries Management Division, Alaska Fisheries Science Center, NOAA, NMFS, Seattle, WA, USA

<sup>5</sup>Laboratory for Biological Resources of the Far-Eastern and Arctic Seas, Pacific branch of the Russian Federal Research Institute Of Fisheries and Oceanography VNIRO (TINRO), Vladivostok, Russia

## Correspondence

Lukas B. DeFilippo, Resource Assessment and Conservation Engineering Division, Alaska Fisheries Science Center, NOAA, NMFS, Seattle, WA, USA.  
Email: [lukas.defilippo@gmail.com](mailto:lukas.defilippo@gmail.com)

## Present address

Lukas B. DeFilippo, Ecosystem Monitoring and Assessment Program, Alaska Fisheries Science Center, Seattle, WA, USA.

## Funding information

North Pacific Research Board, Grant/Award Number: 1805

## Abstract

Many mobile marine taxa are changing their distributions in response to climate change. Such movements pose a challenge to fisheries monitoring and management, particularly in systems where climate-adaptive and ecosystem-based management objectives are emphasized. While shifts in species distributions can be discerned from long-term fisheries-independent monitoring data, distilling coherent patterns across space and time from such datasets can be challenging, particularly for transboundary stocks. One approach for identifying dominant patterns of spatiotemporal variation that has been widely used in physical atmospheric and oceanographic studies is empirical orthogonal function (EOF) analysis, wherein spatiotemporal variation is separated into time-series of annual factor loadings and spatial response maps. Here, we apply an extension of EOF analysis that has been modified for compatibility with biological sampling data to a combined US–Russian fisheries-independent survey dataset that spans the eastern (United States) and western (Russia) Bering Sea shelf to estimate dominant patterns of spatiotemporal variation for 10 groundfish species at a shelf-wide scale. EOF identified one axis of variability that was coherent with the extent of cold ( $\leq 0^{\circ}\text{C}$ ) near-bottom waters (the cold pool) previously shown to be a key influence on species distributions and ecosystem structure for the Bering Sea. However, the leading axis of variability identified by our EOF analysis was characterized by low frequency changes in the distributions of several species over longer time scales. Our analysis has important implications for predicting variation in species distributions over time and demonstrates a widely applicable method for leveraging combined fisheries-independent survey datasets to characterize community-level responses to ecosystem change at basin-wide scales.

## KEYWORDS

Bering Sea, bottom-trawl, cold pool, distribution shifts, empirical orthogonal function (EOF), groundfish

## 1 | INTRODUCTION

As the oceans warm, many mobile marine taxa are shifting their distributions beyond their historical ranges (Nye et al., 2009; Perry et al., 2005; Pinsky et al., 2013), posing challenges to fisheries monitoring and management (Link et al., 2011; Pinsky et al., 2018). Consequently, characterizing and predicting variation in species distributions over time is often an important objective for scientists and managers (Currie et al., 2019; Karp et al., 2019; Smith et al., 2023). While distributional changes can be discerned from long-term fisheries-independent monitoring datasets, identifying coherent patterns and drivers behind such shifts can be difficult. These challenges are compounded further for transboundary stocks whose movements may extend beyond the extent of any one nation's territorial waters and marine resource surveys. However, there is a growing body of methodology being developed for combining data from multiple nations' fisheries-independent surveys (Maureaud et al., 2021; Moriarty et al., 2020; O'Leary et al., 2021, 2022). Such combined survey datasets not only expand the effective spatial scope of resource monitoring and assessment but also offer opportunities to characterize patterns of variation in species distributions over time and drivers thereof at broader spatial scales.

Dominant spatiotemporal patterns in one or more response variables can be identified using dimension reduction techniques such as empirical orthogonal function (EOF) analysis, which decomposes spatiotemporal variation into separable components of annual indices and spatial response maps. EOF is often applied to physical atmospheric and oceanographic measurements to produce indices that summarize patterns of climatic variation and teleconnections (correlations over broad spatial scales; e.g., the El Niño Southern Oscillation). Recent research has adapted EOF for use with zero-inflated and noisy samples of numerical density for marine organisms (Grüss et al., 2021; Thorson et al., 2021; Thorson, Cheng, et al., 2020; Thorson, Ciannelli, & Litzow, 2020), in which the resulting indices represent dominant patterns of variation in species distributions over time. Such models can be applied to biological survey data and can accommodate multispecies datasets to make inferences at the community level. However, EOF has yet to be adapted for combining fisheries-independent survey datasets from multiple countries to identify basin-scale patterns of variation in transboundary species assemblages.

The Bering Sea shelf is a transboundary ecosystem that spans the territorial waters of the United States to the east and the Russian Federation to the west. As the basis for many valuable fisheries, the Bering Sea has been studied heavily, and the oceanography of this region is well characterized, as are the mechanisms linking environmental conditions to biological outcomes via bottom-up effects (e.g., Danielson et al., 2011; Hunt et al., 2011; Stabeno et al., 2001; Wyllie-Echeverria & Wooster, 1998). Similarly, research has identified top-down drivers (e.g., predation and fishing) of population and community dynamics in the Bering Sea that are important for fisheries assessment and management (Aydin & Mueter, 2007; Holsman et al., 2016). Much of the research that informs these frameworks has

focused on the US (southeastern, northeastern) or Russian (western) shelf areas separately, often with the goal of understanding and predicting variation in the distribution and abundance of fish stocks within each country's waters (Grüss et al., 2021; Hunt et al., 2011; Mueter et al., 2006; Stabeno et al., 2001; Stepanenko & Gritsay, 2016; Thorson, 2019). However, substantial warming and sea ice loss in the Bering Sea are causing changes in species' distributions, resulting in northward shifts (Mueter & Litzow, 2008; Spies et al., 2020; Stevenson & Lauth, 2019) and increased movements between the eastern and western shelves in some cases (Eisner et al., 2020). As such, the spatial scope of environmental and ecological processes affecting fish populations in this region may be evolving, making it increasingly important to consider the biophysical and community dynamics of the Bering Sea at a broader, shelf-wide scale.

Efforts to track changing species distributions by combining fisheries-independent survey data are underway in several regions and are proving useful for expanding the effective spatial coverage of monitoring (Maureaud et al., 2021; Moriarty et al., 2020; O'Leary et al., 2021). However, these combined datasets have seldom been leveraged to explore patterns of variation in stock dynamics and oceanographic or ecological drivers thereof at broader scales. Moreover, variation in fish and invertebrate distributions in the Bering Sea are strongly linked to environmental conditions, suggesting the possibility for coherent patterns of spatiotemporal variation among species that may not be evident from single-species analyses. Here, we apply an extension of EOF analysis (Thorson, Ciannelli, & Litzow, 2020) to a combined multispecies US–Russian fisheries-independent survey dataset to identify dominant axes of spatiotemporal variability for Bering Sea groundfishes at a shelf-wide scale. We found one axis of variability that is coherent with the spatial extent of cold ( $\leq 0^{\circ}\text{C}$ ) near-bottom waters (the cold pool) known to be a key influence on species distributions and ecosystem dynamics in the Bering Sea (Eisner et al., 2020; Kotwicki & Lauth, 2013). However, the primary axis of variability identified by our analysis was associated with sustained, low frequency changes in the distributions of several species. Further analyses using spatially-varying coefficient models and range shift metrics corroborated the patterns identified by EOF. Our findings have useful applications for characterizing and predicting species distribution shifts in the Bering Sea, and our analysis demonstrates a generic approach for leveraging combined fisheries-independent survey datasets to understand community-level responses to ecosystem change at broader scales.

## 2 | METHODS

The goal of this study is to use combined fisheries-independent survey data that span the southeastern (EBS), northeastern (NBS), and western (WBS) Bering Sea shelves to characterize patterns of spatiotemporal variation for Bering Sea groundfish at a shelf-wide scale. Our analysis proceeds in three general stages: (1) using exploratory EOF to identify dominant axes of variability for the groundfish assemblage represented in our data set, (2) comparing these estimated

axes to an oceanographic index known to influence species distributions in the Bering Sea (cold pool extent), and (3) further investigating patterns indicated by exploratory EOF using a confirmatory factor model (*sensu* Grüss et al., 2020; i.e., with spatially varying coefficient [SVC] models), and range shift metrics.

## 2.1 | Study region and survey extents

The fisheries-independent survey data analyzed in this study include coverage of the EBS, NBS, and WBS subregions. The EBS is defined here as the section of the Bering Sea southeast of the US–Russian international maritime boundary and spans from Bristol Bay and the Alaska Peninsula to the south, to north of Nunivak and St. Matthew Island (Figure 1). The EBS shelf is often viewed as being comprised of three distinct domains defined by bathymetric and oceanographic conditions: the inner domain (0–50 m), middle domain (50–100 m), and outer domain (100–200 m) (Coachman, 1986; Kinder & Schumacher, 1981; Figure 1). The NBS, as defined here, also occurs in US territorial waters and spans from north of Nunivak and St. Matthew Island up to Norton Sound and the Bering Strait (Figure 1). The NBS is generally shallower (<100 m) and bathymetrically homogenous compared with the EBS. West of the international maritime border in Russian territorial waters, the WBS spans from the western Bering Strait, the Chukotka Peninsula and Anadyr Bay to the north, and Cape Navarin and the Koryak shelf to the south (Figure 1).

The area we define as the WBS in our study includes a broad range of depths, including several areas exceeding 200 m (Figure 1).

## 2.2 | Fisheries-independent survey data

The primary EBS and NBS data used in this study are presence-absence and biomass measurements collected from fishery-independent bottom trawl surveys conducted by the US National Oceanic and Atmospheric Administration's (NOAA) Alaska Fisheries Science Center (AFSC). The EBS survey occurs annually from May to early August and samples a fixed set of 376 stations as part of a systematic design with a minimum grid resolution of 37.04 km<sup>2</sup> and a maximum depth of 200 m (Lauth et al., 2019). Sampling for the EBS survey begins in the southeast corner of the survey extent (Bristol Bay) and proceeds west using two chartered commercial vessels. Each vessel tows a standard 83'–112' eastern otter trawl with 10-cm mesh for a 30 min at a target speed of 3 knots (Lauth et al., 2019). Survey effort is measured as the area-swept, calculated as the product of the distance fished (measured duration of seafloor contact measured using a GPS and a bottom contact sensor), and net width measured using an acoustic sensor. A total of 12 vessels have been used during the time-period considered in this study.

The NBS survey follows the same sampling design and protocol as the EBS survey but occurs later in the year, from early August to September. Additionally, the frequency and spatial extent of the NBS

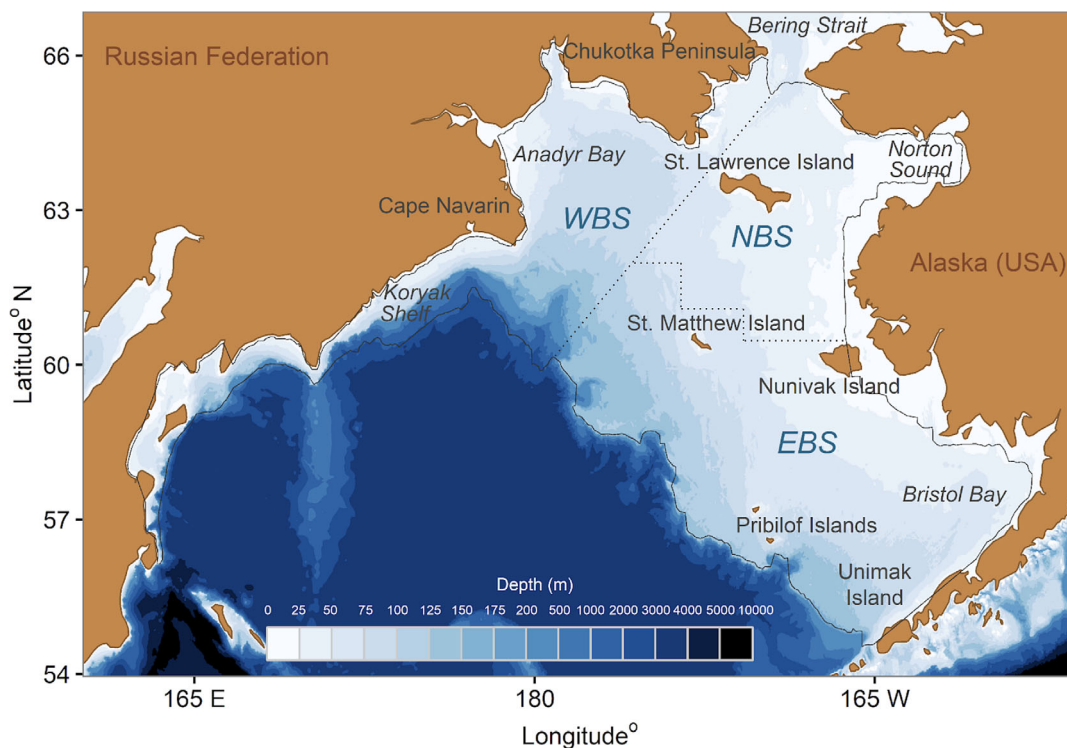


**FIGURE 1** Map of the Bering Sea and associated features. The spatial extent of all survey data analyzed in this study is indicated by the outer gray boundary. Subregions, as defined in the text, are delineated by the dotted gray lines demarcating the western (WBS), southeastern (EBS), and northeastern (NBS) shelf regions.

survey have been more irregular than the EBS survey, with partial sampling of the NBS survey extent occurring in 1982, 1985, 1988, 1991, 1994, 2001, 2005, 2006, and 2018, and full sampling in 2010, 2017, and 2019 (Lauth et al., 2019).

All WBS data were collected from fisheries-independent bottom trawl surveys conducted by the Pacific Branch of the Russian Federal Research Institute of Fisheries and Oceanography (TINRO). Sampling of the WBS has occurred from 1982 to 2017 throughout all months of the year, but primarily from May to August (O'Leary et al., 2021). The WBS survey does not follow a probabilistic sampling design, and the timing and spatial extent of the survey are variable. Vessels typically tow for 30 min at 3.2 knots, although tow duration ranged from 0.08 to 24 h (O'Leary et al., 2021). A total of 32 unique vessels have been used to conduct the survey throughout the time period considered in this study. Importantly, TINRO also surveyed the EBS shelf from 1982 to 1991 as part of a cooperative sampling effort between NOAA and TINRO ([https://apps-afsc.fisheries.noaa.gov/RACE/surveys/cruise\\_archives/cruises1983/results\\_AK-CH1983-01\\_03.pdf](https://apps-afsc.fisheries.noaa.gov/RACE/surveys/cruise_archives/cruises1983/results_AK-CH1983-01_03.pdf); Volvenko et al., 2018), which facilitates the estimation of catchability ratios (Section 2.4.1) between the AFSC and TINRO surveys needed to combine these disparate data sources (O'Leary et al., 2021, 2022). The species included in our study were selected based on criteria of life history and taxonomic representation as well as sufficient abundance in the catch data—particularly during years in which TINRO surveyed the EBS—to allow estimation of species-specific catchability ratios. Such catchability ratios have been previously estimated for Pacific cod, *Gadus macrocephalus*, Alaska plaice, *Pleuronectes quadrituberculatus*, and walleye pollock, *Gadus chalcogrammus* by O'Leary et al. (2021, 2022) but not for the other seven species in our analysis: Greenland turbot, *Reinhardtius hippoglossoides*, Pacific halibut *Hippoglossus stenolepis*, flathead sole, *Hippoglossoides elassodon*, yellowfin sole, *Limanda aspera*, northern rock sole, *Lepidopsetta polyxystra*, yellow Irish lord, *Hemilepidotus jordani*, and great sculpin, *Myoxocephalus polyacanthocephalus*.

### 2.3 | The cold pool index

Given the well-documented importance of the cold pool in the Bering Sea, we are particularly interested in whether dominant axes of variability estimated at a shelf-wide scale (EBS + NBS + WBS) are coherent with cold pool extent. The formation of winter (approximately mid-December) sea ice in the Bering Sea creates a layer of cold, saline water that sinks to the seafloor and forms the cold pool. While the cold pool is conventionally defined as the area of waters 2°C or colder (Wyllie-Echeverria & Wooster, 1998), there is evidence that the 0°C isotherm may be more influential in shaping species distributions (Kotwicki & Lauth, 2013). The presence of sea ice in the spring limits water column mixing, and the resulting stratification restricts heat exchange between the cold pool and the warming surface waters (Stabeno et al., 2012; Wyllie-Echeverria & Wooster, 1998). Consequently, the cold pool can persist into the summer at a size determined by the extent and phenology of sea ice

(De Robertis & Cokelet, 2012; Hollowed et al., 2012; Stabeno et al., 2012). For instance, in warm years associated with reduced ice coverage and earlier (i.e., before early March) ice retreat, the extent of the cold pool may be minimal and restricted to the northern portion of the middle domain (50–100 m isobath) (Hollowed et al., 2012; Stabeno et al., 2010). Conversely, in colder years where sea ice extent is larger and persists through April, the cold pool may extend farther south and occupy much of the middle shelf (Stabeno et al., 2001; Wyllie-Echeverria & Wooster, 1998). The cold pool is thought to act as a barrier to the movements of subarctic fishes, restricting northward and cross-shelf migrations (Eisner et al., 2020; Kotwicki et al., 2005; Stabeno et al., 2012). As such, the spatial extent of the cold pool is a key influence on the distributions of many subarctic fish and invertebrate species (Ciannelli & Bailey, 2005; Mueter & Litzow, 2008; Thorson, 2019; Thorson, Ciannelli, & Litzow, 2020). Furthermore, cold pool size is directly or indirectly associated with variation in circulation patterns (Stabeno et al., 2012) the timing and magnitude of primary production (Stabeno et al., 2002, 2007, 2010), zooplankton community composition (Coyle et al., 2011; Sigler et al., 2016), and predator–prey overlap (De Robertis & Cokelet, 2012; Grüss et al., 2020), and thus serves as a useful proxy for ecosystem conditions. However, much of the research exploring the effect of the cold pool on species distributions and ecosystem dynamics has focused on particular subregions (e.g., the EBS), and less is known about how the Bering Sea responds to variation in the cold pool at a shelf-wide scale (but see Eisner et al., 2020).

We compared axes of variability identified by exploratory EOF (Section 2.4.1) with annual measurements of the cold pool extent and calculated Spearman's correlation coefficient ( $\rho$ ) for each relationship. We also directly estimated the effects of the cold pool on each species' spatiotemporal dynamics at the shelf-wide scale using SVC models (Section 2.4.2). Data on cold pool extent used in these analyses were the measured spatial extent in square kilometers (km<sup>2</sup>) of bottom temperatures 0°C or colder based on temperature measurements recorded on AFSC surveys. We use a 0°C threshold here based on previous evidence that some fish species (i.e., walleye pollock) do not form feeding aggregations in waters below this temperature in the EBS (Baker, 2021) and that 0°C may be a more important temperature threshold affecting groundfish distributions (Kotwicki & Lauth, 2013).

It is important to note that the measured cold pool area used in this study is based on annual NOAA bottom trawl survey data and thus confined to the southeastern Bering Sea shelf (EBS). While the area occupied by the cold pool can extend into the WBS and NBS, consistent measurements of bottom temperatures in these areas were not available for much of the focal time period of this study. As such, we use the measured cold pool area in the EBS as a proxy for the total cold pool area across the Bering Sea shelf (EBS, NBS, and WBS). While our measurements of cold pool area do not encompass the full spatial extent of our study area, we assume that the cold pool area in the EBS is correlated with that of the WBS and NBS (Eisner et al., 2020), although there may be incongruences that bear consideration when interpreting our results.

## 2.4 | Model descriptions

All models used in this study follow a spatiotemporal design implemented using the vector autoregressive spatiotemporal (VAST) package (release number 3.9.0) (Thorson & Barnett, 2017) in R-4.0.3 (R Core Team, 2015). The exploratory EOF model was fit to data for all species simultaneously, while single-species specifications were used for the SVC model (2.4.2) and calculation of range shift metrics (2.4.3). While the EOF model was intended to identify patterns across species at the assemblage level, the range shift metrics and SVC models were intended to make inferences for individual species and thus a single-species specification was more suitable. To account for differences in sampling efficiency between the AFSC and TINRO surveys, we implemented the method of O'Leary et al. (2022), which specifies a spatially invariant catchability covariate on both linear predictors ( $Q_i$ ) for each species representing the log-ratio of expected catch for the TINRO survey relative to the AFSC survey if they occurred at the same time and place and with the same area-swept.

### 2.4.1 | Exploratory EOF

EOF is a rank reduction approach with a long history of use in physical oceanographic and atmospheric studies (Grimmer, 1963; McGowan et al., 1998). Several well-known metrics of atmospheric and oceanographic variation such as the El Niño Southern Oscillation (ENSO, Kidson, 1975) and Pacific Decadal Oscillation (PDO, Mantua et al., 1997) are products of EOF analysis applied to spatiotemporal physical oceanographic and atmospheric measurements. EOF operates by taking values of one or more response variables measured across space and time and identifying dominant axes (factors) of variability in the response variable(s), which are expressed as time-series representing each year's association (loading) with a given factor (Thorson, Ciannelli, & Litzow, 2020). These time-series are accompanied by a spatial 'response map', which shows how variables at each location respond to interannual variation in that axis. For example, the PDO index is derived from EOF analysis of monthly sea surface temperature anomalies (Mantua et al., 1997). The PDO index varies in magnitude and phase (positive vs. negative) over time, which represent each year's loadings onto this factor. Positive phases of the PDO are associated with cooler sea surface temperatures in the interior North Pacific, warmer temperatures along the Pacific coast, and below-average sea level pressure over the North Pacific (Mantua et al., 1997), which represents the spatial response maps for this axis of variation. In other words, the response maps for the PDO are characterized by negative coefficients for temperature in the interior North Pacific, positive coefficients for temperature along the Pacific coast, and negative coefficients for sea level pressure over the North Pacific.

The exploratory EOF model used here is an extension of conventional EOF that has been modified for applicability to biological sampling data (Grüss et al., 2021; Thorson et al., 2021; Thorson,

Cheng, et al., 2020; Thorson, Ciannelli, & Litzow, 2020) and follows spatiotemporal design implemented in VAST. VAST models follow a generalized linear mixed model framework that approximates the dependent variable(s) of interest using a link function and two linear predictors. Variation in the response variable(s) over space and time is decomposed into three components: (1) temporal variation ( $\beta$ ), which represents changes from year-to-year that are expressed equivalently among all locations, (2) spatial patterns ( $\omega$ ), which correspond to unmeasured variation over space that is stable over time and represents long-term habitat associations, and (3) spatiotemporal variation ( $\epsilon$ ), which represents changes from year-to-year that differ across locations. Biological data present analytical challenges not posed by the atmospheric or oceanographic measurements to which EOF is typically applied, such as the presence of many zeros, skewed distributions, and spatially unbalanced sampling. As such, the EOF extension used here was implemented using a Poisson-link delta modeling approach with two estimated linear predictors,  $n$  and  $w$ , which represent expected numerical density and biomass-per-individual respectively such that  $n_i w_i$  gives the expected biomass density ( $d_i$ ) of sample (survey haul)  $i$  (Thorson, 2018):

$$\begin{aligned}\log(n_i(c_i)) &= \beta_1(c_i, t_i) + \omega(c_i, s_i) + \sum_{f=1}^{N_f} \lambda(t_i, f) \epsilon(s_i, c_i, f) + \gamma_1(c_i) Q_i \\ \log(w_i(c_i)) &= \beta_2(c_i, t_i) + \gamma_2(c_i) Q_i,\end{aligned}\quad (1)$$

where  $s_i$  and  $t_i$  are the location and year associated with sample  $i$ . The estimated catchability coefficients ( $\gamma_1(c_i), \gamma_2(c_i)$ ) varied by species and described the log sampling efficiency of the TINRO surveys relative to the AFSC surveys via the catchability covariate ( $Q_i$ ). Following O'Leary et al. (2022), Catchability covariates were implemented as categorical variables denoting the agency that collected each sample ( $i$ ) with the AFSC surveys defined as the reference category ( $Q_i = 0$ ). Thus, the combined effects of the catchability coefficients ( $e^{\gamma_1(c_i)} e^{\gamma_2(c_i)}$ ) represent the catchability ratio of the TINRO survey relative to the AFSC surveys. The annual intercepts ( $\beta_1(c_i, t_i), \beta_2(c_i, t_i)$ ) were specified as fixed effects that are independent among years, and the spatial variation terms ( $\omega$ ) were estimated as random effects following a multivariate normal distribution:

$$\omega(c) \sim \text{MVN}(0, \sigma_\omega^2 \mathbf{R}(\eta)), \quad (2)$$

where  $\sigma_\omega^2$  is the marginal spatial variance and  $\mathbf{R}(\eta)$  is the correlation matrix among locations ( $s$ ), which follows a Matérn function with decorrelation distance of  $\eta$  and a transformation matrix that allows for geometric anisotropy such that decorrelation distance varies with cardinal direction (Thorson et al., 2015). A defining characteristic of EOF lies in the specification of spatiotemporal variation as the product of annual factor loadings ( $\lambda(t_i, f)$ ) and a spatial response map associated with each factor for each category (species in our case) ( $\epsilon(s_i, c_i, f)$ ). Here,  $\lambda(t_i, f)$  represents the loadings ( $\lambda$ ) between each year ( $t$ ) and factor ( $f$ ) based on the estimated loadings matrix  $\Lambda$ . The annual loadings represent the magnitude and sign of a given year's association with a given factor. The response map associated with

each factor ( $\epsilon(c,f)$ ) follows a multivariate normal distribution specified similarly to the spatial variation terms (Equation 2):

$$\epsilon(c,f) \sim \text{MVN}(0, \sigma_\epsilon^2 \mathbf{R}(\eta)), \quad (3)$$

where  $\sigma_\epsilon^2$  represents the marginal spatiotemporal variance.

The encounter probability for a given species in sample  $i$  ( $p_i(c_i)$ ) can be derived as a complementary log-log link from the log-numerical density ( $\log(n_i)$ ), which represents the probability of encountering one or more individuals that are drawn from a Poisson distribution with intensity  $n_i$ :

$$p_i(c_i) = 1 - \exp(-n_i(c_i)). \quad (4)$$

Similarly, the expected biomass given a positive encounter  $r_i(c_i)$  for sample  $i$  is obtained from the numerical density and average biomass per individual ( $w_i(c_i)$ ) as

$$r_i(c_i) = \frac{n_i(c_i)}{p_i(c_i)} w_i(c_i). \quad (5)$$

The probability of the biomass data is then assumed to follow a lognormal distribution such that

$$\Pr(b_i(c_i) = B) = \begin{cases} 1 - p_i(c_i), & B = 0 \\ p_i(c_i) \times \text{Lognormal}(B, \log(r_i(c_i)), \sigma_r^2(c_i)), & B > 0 \end{cases} \quad (6)$$

where  $1 - p_i$  is the probability mass associated with a biomass of zero, and  $\text{Lognormal}(B | \log(r_i(c_i)), \sigma_r^2(c_i))$  is the lognormal probability of biomass  $B$  given an expected biomass for positive encounters of  $r_i$  and residual lognormal variance  $\sigma_r^2(c_i)$ .

To ensure identifiability, constraints must be placed on the loadings matrix ( $\Lambda$ ). Specifically,  $\lambda(t, f)$  were fixed to zero for all values of  $t > f$ , and we imposed a constraint that the loadings for a given factor must sum to zero (i.e.,  $\sum_{t=1}^{N_t} \lambda(t, f) = 0$ ) where  $N_t$  is the number of years. The zero-centering constraint on annual factor loadings ensures that spatiotemporal variation is separable from spatial variation such that in a hypothetical 'average' year (i.e., where  $\lambda(t, f) = 0$ ), all variation across space is attributable to  $\omega$ . After estimation, the loadings matrix is rotated for interpretability using a rotation matrix  $\mathbf{P}$ , defined such that the columns of  $\Lambda \mathbf{P}$  are identical to the eigenvectors of  $\Lambda^T \Lambda$ . Thus,  $\Lambda \mathbf{P}$  is defined as the factor index and  $\Lambda \epsilon$  as the realized spatial response (Thorson, Ciannelli, & Litzow, 2020). This 'PCA rotation' maximizes each axis of variability in sequential order, such that the first axis explains the most variation (Thorson, Ianelli, et al., 2016), analogous to how axes are defined in conventional EOF analysis.

## 2.4.2 | SVC model

The purpose of the SVC model used here is to estimate the spatially varying effect of the annual cold pool extent and calculate the amount

of variance that this covariate explains for each species. SVCs for cold pool extent were included on both linear predictors ( $\xi_1(s), \xi_2(s)$ ), representing the predicted impacts of the covariate on both numbers density ( $n_i$ ) and average biomass ( $w_i$ ). Note that the specification of the linear predictors under the SVC model differs from that of the EOF described in Section 2.4.1 and a full description can be found in Thorson (2019). Coefficients for each species were specified as a zero-mean Gaussian Markov random field with unit variance and the annual cold pool area measurements were z-score transformed prior to model fitting (i.e., subtracting the mean and dividing by the standard deviation). We calculated the percent variance explained (PVE) by the cold pool covariate for each species by comparing the residual spatiotemporal variance between a model with the cold pool extent covariate ( $\sigma_\epsilon^2$ ) and a null model without this covariate ( $\sigma_{\epsilon_0}^2$ ) following Thorson (2019; appendix C):

$$\text{Percent variance explained (PVE)} = 1 - \frac{\sigma_\epsilon^2}{\sigma_{\epsilon_0}^2}. \quad (7)$$

Additionally, we calculated the percent deviance explained by the entire model by comparing the deviance of the fitted model to that of a null model without any spatial or spatiotemporal random effects or covariates.

## 2.4.3 | Range shift metrics

When applied to biological sampling data, axes of variability identified by exploratory EOF analysis represent patterns of variation in species distributions over time. To further investigate and interpret such patterns, we also directly quantified changes in species distributions by estimating the center of gravity of each species' biomass. Center of gravity was calculated with respect to both latitude ( $m=1$ ), and longitude ( $m=2$ ) as the centroid of the population distribution ( $Z(t, m)$ ), or the mean location weighted by population density:

$$Z(t, m) = \frac{\sum_{s=1}^{n_s} z(s, m) a(s) d(s, t)}{I(t)}, \quad (8)$$

where  $d(s, t)$  is the predicted population density at location  $s$ , and time  $t$ ,  $a(s)$  is the area associated with location  $s$ , and  $z(s, m)$  is coordinate of location  $s$  (in latitude if  $m=1$ , longitude if  $m=2$ ) for which center of gravity is calculated, and  $I(t)$  is the biomass index (across the entire study area) in year  $t$ . Additional details on center of gravity calculations can be found in Thorson, Pinsky, and Ward (2016).

## 2.4.4 | Model estimation and validation

Spatial variables were estimated as random effects following a Gaussian Markov random field. A specified number of 'knots' were arranged to minimize the distance between the sampling locations and knots using a  $k$ -means algorithm. A stochastic partial differential

equation approach was then used to generate a triangulated mesh with a vertex at each knot. The correlation between locations within the triangular mesh approximates a Matérn function. The value of a spatial variable at any given location within the mesh was calculated as the weighted average of the three surrounding vertices using bilinear interpolation. The spatial domain was defined using a WGS84 projection.

Fixed effects were estimated by identifying their values that maximized the marginal likelihood via automatic differentiation (Fournier et al., 2012). The marginal likelihood itself was calculated when integrating the joint likelihood across values of the random effects via Laplace approximation (Skaug & Fournier, 2006) as implemented in the TMB R package (Kristensen et al., 2020). The gradient of the approximated marginal log-likelihood was then minimized within the R environment. Model convergence was assessed by verifying that the gradients of all parameters were  $<0.001$ . Center of gravity estimates (Section 2.4.3) were also epsilon bias corrected (Thorson & Kristensen, 2016) to account for re-transformation bias.

Model fits were evaluated using simulation-based probability-integral-transform (PIT) residuals (Smith, 1985; Warton et al., 2017) via Q-Q plots and spatial residual visualizations available in the DHARMA package (Hartig, 2022). Diagnostic objects for the simulation-based quantile residuals were generated by sampling from the predictive distribution of a model's fixed and random effects, and calculating and plotting the PIT residuals between the observed and simulated values (Figure S1).

## 3 | RESULTS

### 3.1 | Spatial patterns: EBS and NBS

Within the US portion of the Bering Sea shelf, estimates of  $\omega$  indicated areas of consistently high relative biomass on the inner shelf (0–50 m depth contour, Figure 1) for nearshore species such as yellowfin sole, while the deeper dwelling Greenland turbot were negatively associated with this area (Figure 2). Pacific cod and great sculpin each showed comparatively diffuse distributions, with little strongly positive or negative associations with any particular areas of the EBS or NBS shelves (a notable exception being a clear negative association with Norton Sound for both species). Similarly, Pacific halibut showed generally weak spatial associations throughout the EBS and NBS but were less common on much of the northern shelf, particularly around St. Lawrence Island and in Norton Sound. Flathead sole were positively associated with the southern and outer portions of the EBS shelf and strongly negatively associated with much of the NBS. Similarly, yellow Irish lord were positively associated with areas of the southern, outer EBS shelf and negatively associated with the NBS, particularly Norton Sound and the Bering Strait. Walleye pollock showed a strong positive association with the outer and southern portions of the EBS shelf while Alaska plaice were relatively uncommon in the outer EBS shelf and were positively associated with the central EBS and NBS.

### 3.2 | Spatial patterns: WBS

Several notable patterns of species-specific habitat associations emerged for the WBS subregion. Estimates of  $\omega$  for the WBS indicated areas of particularly high walleye pollock densities off Cape Navarin and the central and outer portions of Anadyr Bay. Greenland turbot were also strongly positively associated with the deeper waters in the outer portion of Anadyr Bay and offshore of Cape Navarin and the Koryak shelf. Flathead sole were relatively rare in the shallow (0–25 m depth contour), inshore areas of Anadyr Bay, with positive associations in central and outer Anadyr Bay and off Cape Navarin. As in the EBS, Alaska plaice were relatively uncommon in deeper waters of the WBS, including the areas offshore of Koryak shelf and the southwestern margin of the WBS, with areas of above average density in central Anadyr Bay. Yellowfin sole were also relatively rare in the deeper, southwestern section of the WBS and weakly positively associated with the narrow band of shallow, nearshore habitat in Anadyr Bay. Pacific cod, northern rock sole, and great sculpin showed moderate positive associations throughout Anadyr Bay and the Koryak shelf, while yellow Irish lord were strongly positively associated with the Koryak shelf and the southern WBS. Pacific halibut showed little positive associations anywhere in the WBS but were relatively uncommon in the nearshore sections of Anadyr Bay as well as the western Bering strait and southwest of St. Lawrence Island.

### 3.3 | Axes of variability

In addition to species' long-term spatial associations ( $\omega$ ), we simultaneously estimated axes of variability that are orthogonal to spatial patterns and each other. The first axis of variability estimated by EOF (factor 1) was characterized by low frequency, multidecadal variation (Figure 3). The loadings for factor 1 steadily increase until 2011, after which they decline until the end of the study period (2019). The response maps ( $\epsilon$ ) associated with factor 1 differed among species but showed a common theme of positive responses to the north and/or northwest in several cases (Figure 2). Pollock and cod exhibit this pattern, with positive phases of factor 1 associated with increases for both species in the Bering Strait, Anadyr Bay and near the Chukotka Peninsula, and declines in several areas of the southern outer EBS shelf and between St. Lawrence and St. Matthew islands. Similarly, yellowfin sole, northern rock sole, and Alaska plaice all showed strong positive responses to factor 1 throughout the northern and northwestern shelf, with negative responses in the southern, outer domain of the EBS shelf. Greenland turbot exhibited an area of positive responses to factor 1 within and surrounding Anadyr Bay, with pockets of weakly negative coefficients scattered throughout the southern outer domain of the EBS shelf and around St. Matthew and St. Lawrence islands. Pacific halibut showed generally weak responses to factor 1, with positive coefficients in the northwestern shelf and negative values on the southern outer domain of the EBS. Great sculpin also showed generally weak responses to factor 1, with

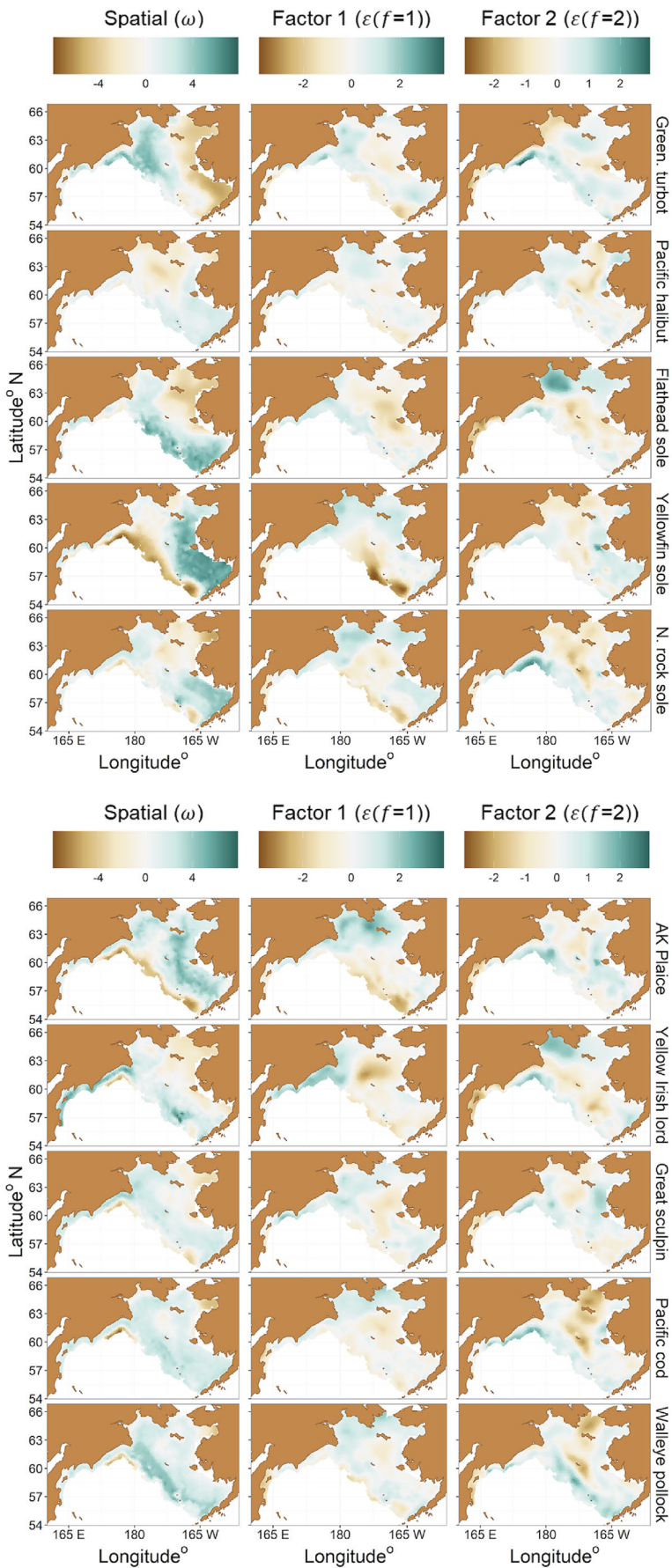


**FIGURE 2** Long term spatial patterns ( $\omega$ ) and response maps associated with EOF factors one ( $\epsilon(f=1)$ ) and two ( $\epsilon(f=2)$ ) by species. Teal and brown areas represent locations of positive and negative coefficient values, respectively, and a value of 0.1 corresponds to an approximately 10% increase in  $n$  or  $w$  relative to the median value of 0.



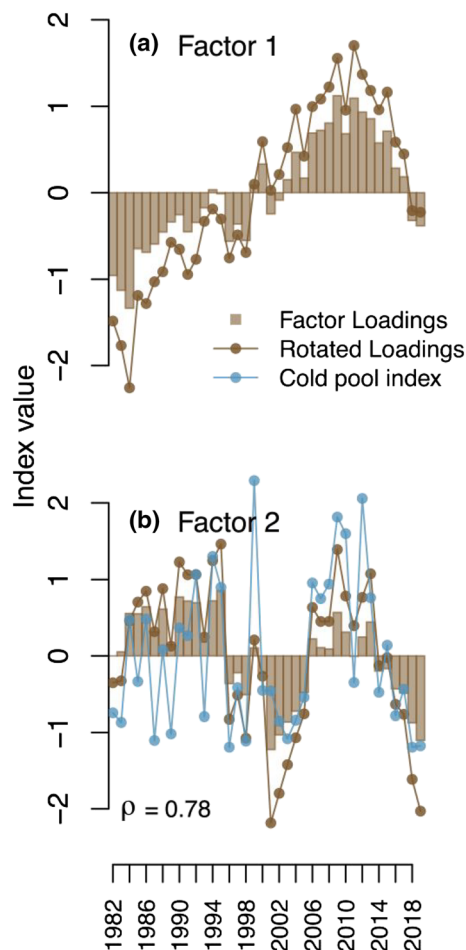


**FIGURE 3** Factor loadings over time. The annual loadings associated with each factor are plotted as brown bars, while the rotated loadings are plotted as brown dots and connected lines. The rotated loadings of the second factor are plotted against the cold pool index (blue) and the Spearman's correlation coefficient ( $\rho$ ) between these indices is reported in the lower left corner of the panel. The cold pool index is z-scored such that the index values represent the number of standard deviations from the mean.

positive coefficient values on the northwestern and southeastern shelf areas and negative values on the outer domain of the EBS and between St. Matthew and St. Lawrence islands. Flathead sole showed declines across a broad area of the eastern shelf near Nunivak, St. Matthew and St. Lawrence islands, and increases on the Koryak shelf and the deeper waters off the Chukotka Peninsula in response to positive loadings of factor 1. Yellow Irish lord showed an area of negative coefficients for factor 1 between St. Matthew and St. Lawrence Islands and the outer margin of the EBS shelf, with a positive response in the westernmost portion of the WBS.

The loadings for the second axis of variability (factor 2) estimated by EOF analysis varied over periods of approximately 1–3 years in the early portion of our study period (1988–1999), transitioning to longer (approximately 5–10 year) stanzas of alternating positive and negative loadings (Figure 3). Visual examination of the rotated loadings and simple correlation analysis indicated that factor 2 closely matches

interannual variation in the cold pool extent ( $\rho = 0.78$ ), with positive and negative loadings corresponding to years of large and small cold pool areas respectively (Figure 3). The spatial response maps associated with factor 2 varied by species but often included negative coefficients between St. Lawrence and St. Matthew islands (Figure 2), an area which is typically occupied by the cold pool when it is present. Both walleye pollock and Pacific cod exhibited this pattern, along with positive responses on the outer EBS shelf. Yellowfin sole and Alaska plaice showed negative responses near St. Matthew and St. Lawrence islands, with positive responses in the inshore areas of the EBS and NBS, and near the Chukotka Peninsula in the WBS. Pacific halibut showed negative coefficients in the area surrounding St. Matthew and St. Lawrence islands in response to factor 2, with weakly positive coefficients throughout the WBS and Norton Sound. Flathead sole and yellow Irish lord showed strong positive responses to factor 2 in Anadyr Bay, with weaker positive responses near St. Lawrence and the Bering Strait, and negative responses throughout much of the central EBS shelf. Northern rock sole showed positive responses to factor 2 on the outer EBS and WBS shelves, with negative responses in the middle and northern shelf areas. Greenland turbot showed areas of positive responses to factor 2 throughout the outer EBS and WBS shelves, as well as surrounding St. Lawrence Island, with an area of negative responses near St. Matthew and Nunivak islands. Great sculpin showed an area of negative response to factor 2 between St. Lawrence and St. Matthew islands and positive coefficients surrounding this area to the east and west.

### 3.4 | Spatially-varying cold pool effect

Similar to the response map for the second EOF factor, the SVCs for cold pool extent were often negative between St. Matthew and St. Lawrence islands (Figure 4), indicating that larger cold pool area was associated with reduced biomass in this area. The coefficient maps and PVE by the cold pool differed substantially among species (Table 1). The cold pool covariate explained the most total spatiotemporal variation for Pacific cod (12.0%), and larger cold pool area was associated with declines around St. Matthew Island for both numbers density and average biomass, as well as increases in average biomass on the southern and outer EBS shelf and parts of the Koryak shelf and Anadyr Bay. (Figure 4). Larger cold pool area was associated with declines in both numbers density and average biomass around St. Matthew Island for walleye pollock and increases in average biomass on the outer EBS shelf and parts of Anadyr Bay and the Koryak shelf. Northern rock sole showed a similar spatial response to the cold pool, with both numbers density and average biomass declining around St. Matthew Island, and average biomass increasing on the southern and outer EBS shelf, as well as in Anadyr Bay. Flathead sole numbers responded negatively to increases in cold pool extent over a relatively large area, particularly around St. Matthew Island and the southern interior of the EBS, while Pacific halibut numbers declined most substantially surrounding and to the east of St. Matthew Island. The cold pool covariate explained comparatively little total

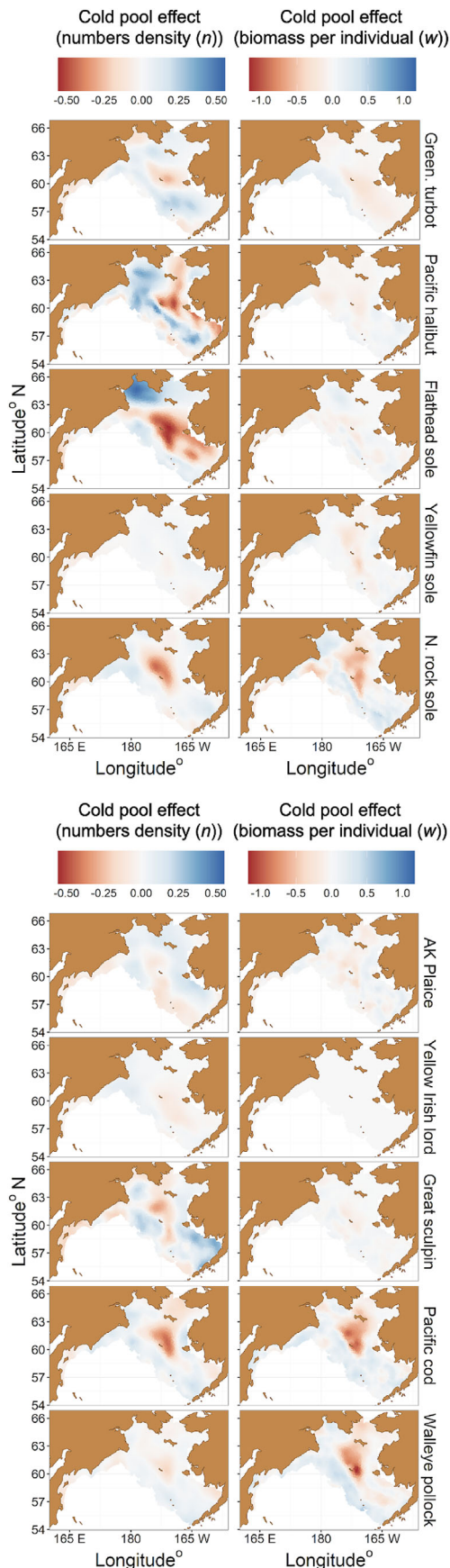


**FIGURE 4** Estimated spatially varying coefficient values for the cold pool extent covariate. The first column shows the estimated effect of cold pool extent on the first linear predictor (numbers density,  $n$ ) and the second column shows effects for the second linear predictor (biomass per individual,  $w$ ).

spatiotemporal variation (<4%) for the other species included in our study (Table 1). It is worth noting that for pollock, cod, and northern rock sole, the cold pool explained more variation for average biomass than numbers density while the opposite was true for flathead sole and Pacific halibut (Table 1).

### 3.5 | Range shift metrics

Estimates of center of gravity over time indicated northward shifts for several groundfish species. Pacific cod began to show signs of northward movement in 2003, reaching a maximum latitude of 61.8 in 2018 (Figure 5). This shift is evident in the distribution of cod biomass density over time as an increase in the Bering Strait and Anadyr Bay (Figure 6). Center of gravity for pollock shows an abrupt shift to the north from 1994 to 1998, followed by a steady northward trend from 2000 to 2019. Similar to cod, northward movement of pollock appears as an increase in biomass density in the Bering Strait and Anadyr Bay over time (Figure 6). Alaska plaice began steadily moving northward relatively early in 1990, reaching a maximum latitude of 61.2 in 2004, and oscillating around a mean latitude of 60.5 from 2004 to 2019. The distribution of biomass density for plaice over time suggests that this northward shift included movements towards central Anadyr Bay and north of St. Lawrence Island (Figure 6). Other species do not show as clear evidence of sustained northward trends or show northward shifts of lower magnitude. For instance, the center of gravity for northern rock sole consistently moved northward from 1982 to 1998, after which it began to shift south from 1999 to 2010, and then north again from 2011 to 2019 (Figure 5). Greenland turbot, Pacific halibut, and flathead sole each exhibited northward trends in their center of gravity during our study period, although of a lesser degree than cod, pollock, and plaice (Figure 5). Northward movements for Pacific halibut appear as a gradual increase in biomass density over time in an area southwest of St. Lawrence Island that this species has historically avoided (Figure 6). Longitudinal trends were much less common, and the magnitude of such movements was generally lower than latitudinal shifts (Figure 5).

## 4 | DISCUSSION

We used exploratory EOF of combined US–Russian fisheries-independent survey data to identify two axes of variability for a Bering Sea groundfish assemblage. The first factor was characterized by low-frequency variation and increased steadily from 1988 to 2011 and then declined moderately until 2019. Species responses to factor

**TABLE 1** Percent variance explained (PVE) by the cold pool extent covariate by species for numbers density (linear predictor 1), biomass per individual (linear predictor 2) and combined across both linear predictors.

| Species            | Numbers density PVE (%) | Biomass per individual PVE (%) | Combined PVE (%) | Percent deviance explained (%) |
|--------------------|-------------------------|--------------------------------|------------------|--------------------------------|
| Greenland turbot   | 1.98                    | 3.84                           | 3.11             | 66                             |
| Pacific halibut    | 10.35                   | 4.85                           | 7.27             | 47                             |
| Flathead sole      | 7.5                     | 3.0                            | 7.24             | 72                             |
| Yellowfin sole     | 0.67                    | 5.15                           | 1.85             | 81                             |
| Northern rock sole | 4.6                     | 9.0                            | 8.67             | 72                             |
| Alaska plaice      | 2.82                    | 4.85                           | 3.78             | 72                             |
| Yellow Irish lord  | 1.15                    | 0                              | 0.10             | 62                             |
| Great sculpin      | 3.55                    | 2.22                           | 3.34             | 52                             |
| Pacific cod        | 6.83                    | 12.27                          | 11.98            | 61                             |
| Walleye pollock    | 3.76                    | 9.38                           | 8.45             | 62                             |

Note: Additionally, the percent deviance explained by the entire model, including covariates, is presented in the far right column.

1 were variable but often included increases in northern and/or north-western areas of the shelf. Additional evidence of such decadal-scale northward distribution shifts was found in estimates of species' center of gravity, which indicated long-term trends towards higher latitudes for several species, particularly Pacific cod, walleye pollock, Alaska plaice, and to a lesser extent, northern rock sole, Pacific halibut, flathead sole, and Greenland turbot. Factor 2 was characterized by interannual variation from 1988 to 1999, followed by alternating stanzas of positive and negative loadings from 2000 to 2019. This second factor was coherent with the measured cold pool extent, and several species' responses were negative in the northern and middle shelf, areas where the cold pool is often present. These results suggest that dominant spatiotemporal patterns for the Bering Sea groundfishes at the shelf-wide scale include short-term responses to cold pool size and lower frequency variation associated with northward movements over multidecadal time scales.

The leading axis of variability identified by EOF was characterized by lower frequency variation that generally increased gradually from 1988 to 2011 and then weakened until 2019. Species responses to this first factor were variable but often included a component of northward movement. This result is not necessarily surprising, as several studies have documented northward distribution shifts in the Bering Sea for several of the species included in this study (Kotwicki & Lauth, 2013; Stevenson & Lauth, 2019; Vestfals et al., 2016). However, such shifts are often attributed to declines in the size of the cold pool, which acts as a barrier to northward migration (Mueter & Litzow, 2008; but see Kotwicki & Lauth, 2013). Conversely, EOF estimated the northward movements associated with the first factor separately from those associated with variation in the cold pool extent, which were represented in the second axis of variability. There are several possible explanations for this result; while cold pool size is an important proximate control of northward migrations, other factors may also contribute to such movements. For instance, cold pool area is correlated with, but not necessarily entirely dependent on, temperature (Thorson, 2019). Indeed, wind and ocean circulation patterns can also affect the size and distribution of the cold

pool independently of temperature (Duffy-Anderson et al., 2017). As such, factor 1 may represent climate-mediated effects on species distribution that are driven by long-term temperature trends not captured in measurements of cold pool area. Similar to our findings, Kotwicki and Lauth (2013) demonstrated that the most important variable explaining northward distribution shifts for groundfish and crab species in the EBS was a 'time lag' effect, representing a long-term temporal trend in species distributions, followed by the effect of cold pool area. Those authors noted that variation in species distribution over time exhibited a northward trend over the 30-year time-series examined while the cold pool fluctuated over shorter time-scales with no indication of a long-term shift. Kotwicki and Lauth (2013) thus concluded that the cold pool could not be solely responsible for the observed distribution shifts. Similarly, Litzow (2017) demonstrated that community-wide patterns of recruitment and species distributions initiated during a prolonged warming period failed to reverse in a subsequent cold stanza, indicating longer term ecosystem shifts not responsive to transient environmental fluctuations. The first factor estimated by our EOF analysis exhibits clear temporal autocorrelation and sustained, low-frequency variation, and may thus be capturing similar dynamics as reported by Kotwicki and Lauth (2013) and Litzow (2017). Indeed, our center of gravity estimates for several species indicated directional trends towards the north, while long-term trends do not appear in the measured cold pool extent. In explaining these northward trends, Kotwicki and Lauth (2013) cited several possible drivers, such as patterns in primary production and in situ light conditions, and greater fishing pressure in the southern EBS due to closer proximity to Dutch Harbor, the area's primary fishing port. In addition to fishing pressure, additional top-down drivers such as predation due to increases in arrowtooth flounder densities on the EBS shelf (Zador et al., 2011) and northern fur seal colonization of Bogosloff Island in the 1980s (Loughlin & Miller, 1989) may also be contributing to northward trends in groundfish distributions. Without knowing the mechanism(s) responsible for creating the dynamics indicated by factor 1, it is difficult to interpret the decline in the loadings for this factor from 2011 to 2019. However, this period of relaxation

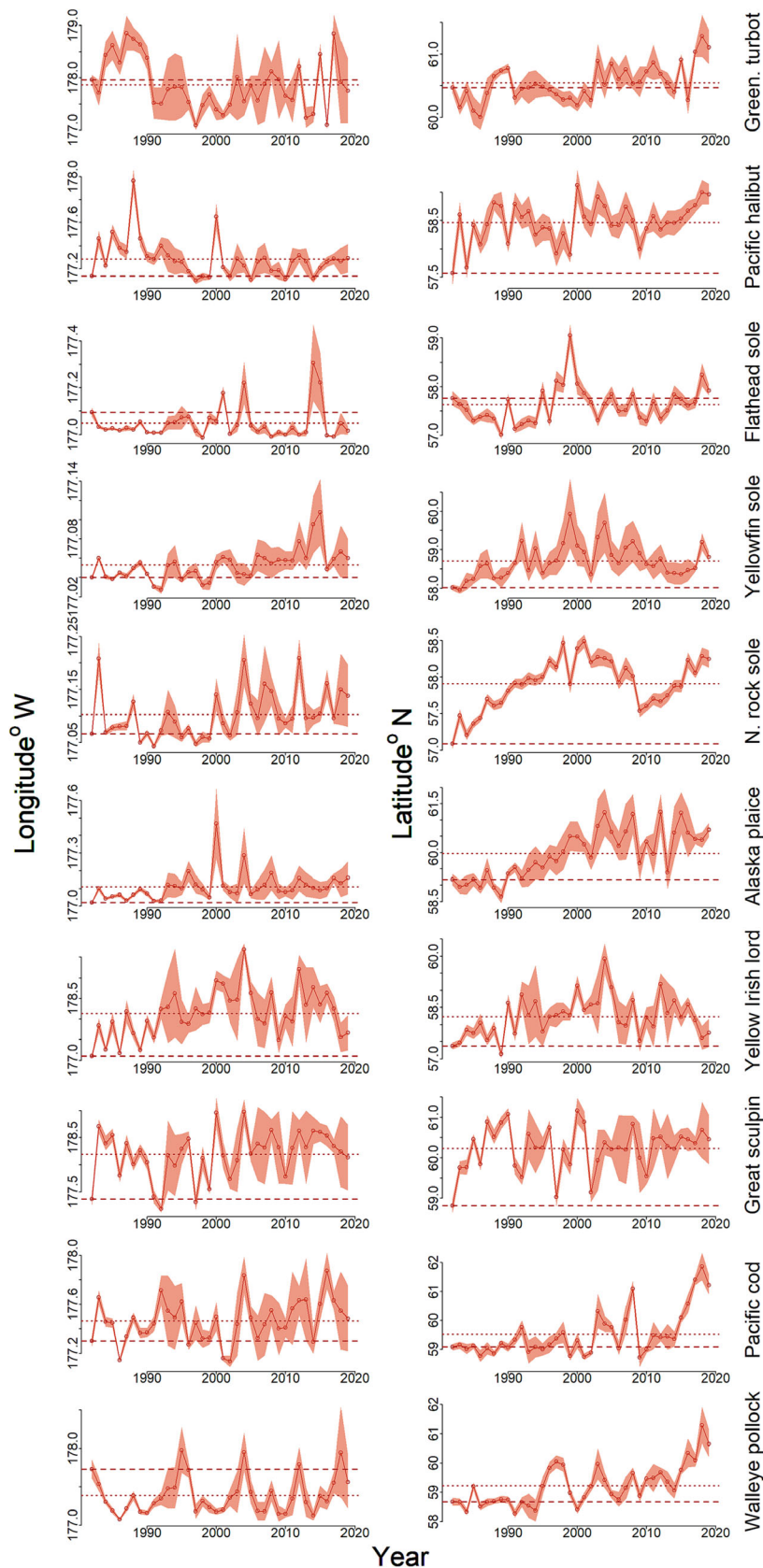
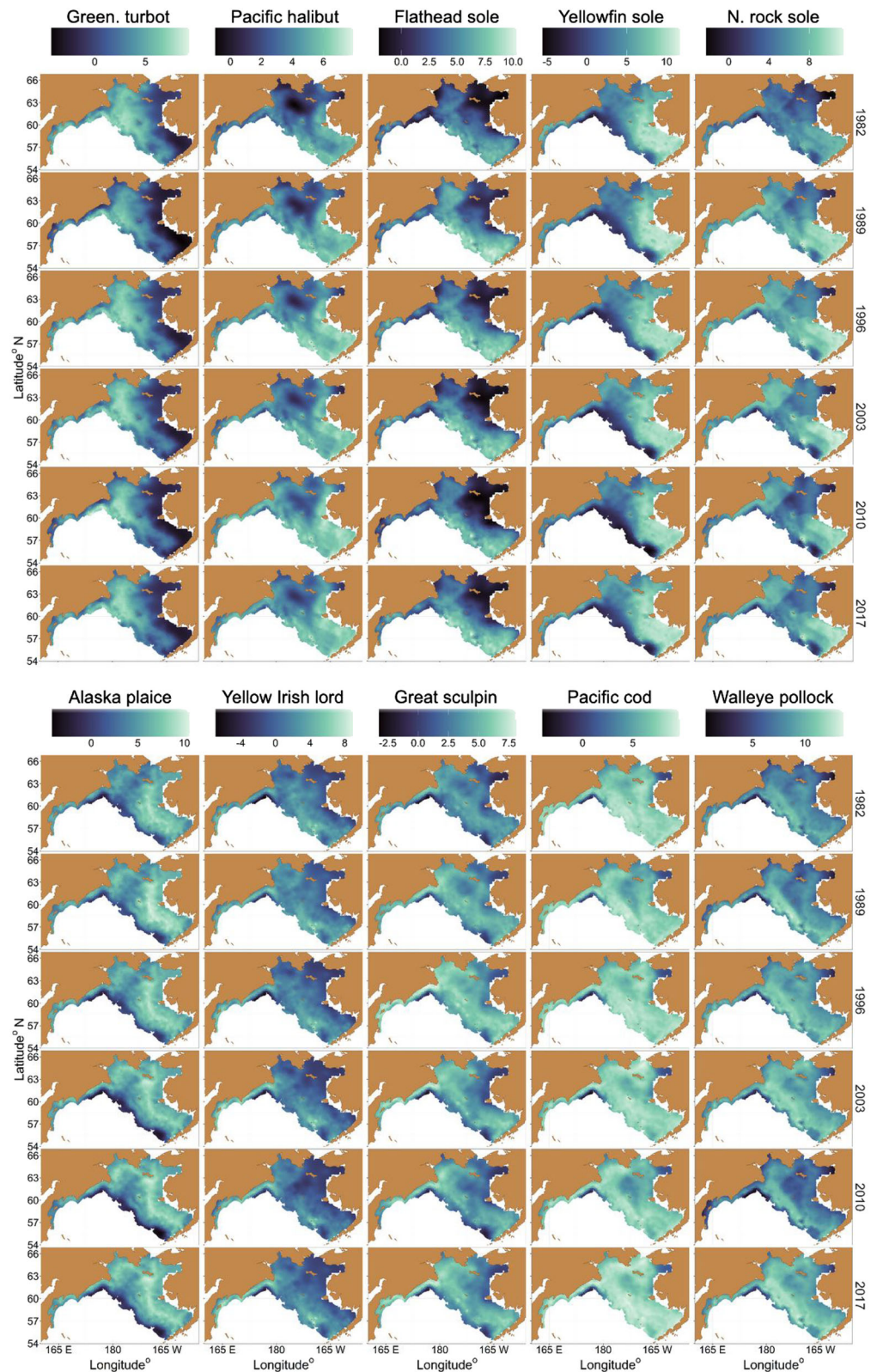


**FIGURE 5** Estimated centers of gravity by latitude (right column) and longitude (left column) for each species over time. Shaded boundaries represent the standard errors associated with estimates. Dashed horizontal lines represent the first value associated with each estimate, and dotted lines represent the mean center of gravity estimate across the entire study period (1982–2019).

in factor 1's loadings coincides roughly with a period of steep decline in cold pool area due to sea ice loss (Figure 3), which led to pronounced changes in the Bering Sea ecosystem (Duffy-Anderson

et al., 2017; Duffy-Anderson et al., 2019; Stabeno & Bell, 2019). As such, the weakened loadings for factor 1 during this period may represent the influence of unprecedented declines in sea ice and cold pool

**FIGURE 6** Spatial distribution of log biomass density in kilograms per kilometer ( $\log [kg/km^2]$ ) by species over time. The distribution of log biomass density for species in years 1982, 1989, 1996, 2003, 2010, and 2017 is shown in each column.



area effectively overriding other mechanisms (i.e., factor 1) that had been shaping variation in species distributions. Whatever the causes, it is evident that there is a low-frequency, multidecadal component to groundfish movements in the Bering Sea that is not explained by the

cold pool and should be accounted for in modeling and predicting species distributions shifts.

Given its well-documented importance in the Bering Sea, it is not surprising that cold pool area corresponded to the second axis of

variation we identified. Indeed, spatial coefficients associated with both factor 2 (exploratory EOF) and the cold pool covariate (SVC models) were characteristic of previously described responses of some species to variation in cold pool extent in the EBS and NBS (e.g., avoidance of the northern and central EBS and NBS to varying extents) (Ciannelli & Bailey, 2005; Mueter & Litzow, 2008; Thorson, 2019; Thorson, Ciannelli, & Litzow, 2020). Species responses to variation in the cold pool for the WBS were often negative west of St. Lawrence Island and in nearshore sections of Anadyr Bay—areas where the cold pool can extend to in the WBS (Eisner et al., 2020; Kearney et al., 2020)—and positive in central and outer Anadyr Bay and the southwestern WBS. Our results support those reported by Eisner et al. (2020) for pollock, which showed that in warm years with smaller cold pool extent, WBS pollock moved northeastward, and EBS pollock moved northwestward, resulting in similar distributions north of St. Lawrence Island. Our results show that other species show a similar spatial response to the cold pool (e.g., cod) and may thus also undergo similar patterns of stock overlap. The importance of the cold pool for shaping the distributions of large mobile species such as pollock and cod has been documented extensively (e.g., Kotwicki et al., 2005; Stevenson & Lauth, 2019; Thorson, 2019). However, our analysis indicates comparably large effects for Pacific halibut, northern rock sole, and flathead sole. Moreover, while yellowfin sole are known to exhibit temperature-mediated variation in the phenology of spawning migrations (Nichol et al., 2019), the estimated effect of the cold pool for this species was relatively small. Not surprisingly, the effects of the cold pool were minor for great sculpin and yellow Irish lord, which are not known to migrate extensively.

This study has several limitations that warrant consideration. While we accounted for differences in sampling efficiency between the AFSC and TINRO surveys in our modeling approach, it is possible that other differences between these disparate data sources (e.g., survey timing and tow duration) could create spurious patterns not corrected by the catchability covariates. However, we note that a similar multispecies EOF analysis limited to the EBS identified axes of variability similar to those described here (Thorson, Ciannelli, & Litzow, 2020), suggesting that incongruences between data sources did not qualitatively affect our results. Our study also did not account for population age and size structure, which can affect both distributional patterns and catchability. For instance, habitat use may be spatially constrained to varying degrees across the life cycle (Ciannelli et al., 2015, 2022), such that some age classes may be more likely to undergo climate-mediated movements (e.g., O'Leary et al., 2020). Thus, aggregating across age classes in our analyses may have obscured ontogenetic patterns in spatial and spatiotemporal variation. Similarly, while we estimated catchability ratios between the AFSC and TINRO surveys by species, interspecific variation in relative catchability is likely driven at least partially by size (O'Leary et al., 2021), and thus may vary intraspecifically with age as well. However, we note that due to the multispecies nature of our EOF analysis, including age and size structure would have been computationally infeasible. Our study also assumed a homogeneous population structure for each species, while in reality, there may be multiple stocks associated with

discrete spawning grounds (e.g., Ianelli et al., 2003) and potential differentiation between shelf areas. While our data were collected in summer and thus lack information on individuals' association with a given spawning population, future tagging and genetic studies (e.g., Spies et al., 2020) would be useful to clarify how population structure may interact with distributional patterns. Finally, it should be noted that the standard errors associated with parts of the EOF response maps described here were substantial (Figure S2), although we corroborated the outcomes of our EOF analysis to some degree via the SVC models and range shift metrics.

As climate-mediated distribution shifts intensify, political cooperation and sharing of survey data can be useful towards understanding how transboundary stocks respond to ecosystem forcing at broader scales, beyond the purview of individual nations. Here, we demonstrate how existing methods for combining fisheries-independent survey data can be leveraged to generate inference on key patterns of variation in species distributions over time via EOF analysis. While our findings are qualitatively similar to a previous EOF analysis limited to the EBS, our inclusion of the NBS and WBS generated novel insights into how species respond to leading axes of variability at a shelf-wide scale. Areas with strong responses to the factors we identified often spanned the US–Russian border, highlighting the shelf-wide coherence of species' responses to ecosystem change. For instance, our analysis demonstrated that some species (e.g., cod and Pollock) show a strong response to reduced cold pool area near the Bering Strait on both US and Russian portions of the shelf. Moreover, given that most of the WBS occurs further north than the EBS, at a similar latitude as the NBS, data from the WBS offers useful insights into characterizing northward distribution shifts. While combining fisheries-independent data from multiple nations' surveys presents both political and analytical challenges, the benefits can be substantial for monitoring and assessment, as well as process-level inferences on species responses to ecosystem change.

Our study identified low-frequency variation often characterized by northward movements, but not associated with cold pool extent, as the leading axis of variation in Bering Sea groundfish distributions over time. While large fluctuations in cold pool area have been associated with conspicuous northward migrations, our findings suggest the co-occurrence of more subtle but persistent northward movements that are less responsive to transient environmental variation, similar to results reported by Kotwicki and Lauth (2013). These results have applications for understanding and predicting species' responses to changing ecosystem conditions. While the cold pool is often viewed as the most important control of northward movements for Bering Sea groundfishes (e.g., Mueter & Litzow, 2008), our study supports Kotwicki and Lauth's (2013) findings that there is another component to such migrations that is not associated with variation in cold pool size. As such, forecasts of species distribution shifts should consider these two patterns operating concurrently across different time scales, as predictions based solely on responses to cold pool size alone may overlook an important component of species movements. Future research identifying the variable(s) responsible for the variation exhibited by factor 1 may further illuminate the mechanisms controlling

shifts in species distributions in the Bering Sea. However, we note that the first EOF axis appears to exhibit distinct autocorrelation, suggesting that it could be usable for short-term forecasts of species distributions even without identifying causal mechanisms. Alternatively, research could identify changes in community structure (i.e., local diversity or predator–prey overlap) associated with positive versus negative phases of the first EOF axis. If these consequences are identified, then it could be useful to include the estimated index itself as an indicator in the eastern Bering Sea Ecosystem Status Report (Siddon, 2022). Collectively, our results emphasize the importance of considering patterns of variation in species distributions across broader spatial scales and demonstrate the utility of EOF applied to combined survey datasets for expanding the spatial scope of process-oriented research.

### AUTHOR CONTRIBUTIONS

Stan Kotwicki, James Thorson, Jerry Hoff, Vladimir Kulik, Andre Punt, Cecilia O'Leary, Lukas DeFilippo, and James Ianelli conceived the study. Lukas DeFilippo conducted the analyses and wrote the paper. All authors contributed to interpreting results and writing the manuscript.

### ACKNOWLEDGMENTS

This research was funded by the North Pacific Research Board (Grant #1805). We thank the many scientific and commercial fishing staff who have contributed to planning and executing surveys in the Bering Sea, and in particular Lyle Britt and Duane Stevenson for their leadership of the eastern Bering Sea team in the NOAA AFSC Groundfish Assessment Program. We would also like to thank M. Stepanenko for their work in the international surveys and I. Glebov and A. Savin for their leadership in coordinating the Russian survey programs. We would also like to thank Sean Rohan, Michael Martin, and Mike Litzow for helpful comments on earlier drafts that improved this manuscript. The scientific results and conclusions, as well as any views or opinions expressed herein, are those of the author(s) and do not necessarily reflect those of NOAA or the US Department of Commerce.

### CONFLICT OF INTEREST STATEMENT

The authors declare no conflict of interest.

### DATA AVAILABILITY STATEMENT

NOAA data are available online (<https://www.fisheries.noaa.gov/alaska/commercial-fishing/alaska-groundfish-bottom-trawl-survey-data#northern-bering-sea-shelf>). All TINRO data are property of the Russian Federation and should be requested through the Federal Agency for Fishery (<http://government.ru/en/department/243/>) and VNIRO (<http://vniro.ru/en/about-vniro/contacts>).

### ORCID

Cecilia A. O'Leary  <https://orcid.org/0000-0002-1737-9294>

Stan Kotwicki  <https://orcid.org/0000-0002-6112-5021>

Vladimir V. Kulik  <https://orcid.org/0000-0003-0920-5312>

### REFERENCES

- Aydin, K., & Mueter, F. (2007). The Bering Sea—A dynamic food web perspective. *Deep Sea Research Part II: Topical Studies in Oceanography*, 54(23–26), 2501–2525.
- Baker, M. R. (2021). Contrast of warm and cold phases in the Bering Sea to understand spatial distributions of Arctic and sub-Arctic gadids. *Polar Biology*, 44(6), 1083–1105. <https://doi.org/10.1007/s00300-021-02856-x>
- Ciannelli, L., & Bailey, K. M. (2005). Landscape dynamics and resulting species interactions: The cod–capelin system in the southeastern Bering Sea. *Marine Ecology Progress Series*, 291, 227–236. <https://doi.org/10.3354/meps291227>
- Ciannelli, L., Bailey, K., & Olsen, E. M. (2015). Evolutionary and ecological constraints of fish spawning habitats. *ICES Journal of Marine Science*, 72(2), 285–296.
- Ciannelli, L., Neuheimer, A. B., Stige, L. C., Frank, K. T., Durant, J. M., Hunsicker, M., Rogers, L. A., Porter, S., Ottersen, G., & Yaragina, N. A. (2022). Ontogenetic spatial constraints of sub-arctic marine fish species. *Fish and Fisheries*, 23(2), 342–357.
- Coachman, L. K. (1986). Circulation, water masses, and fluxes on the southeastern Bering Sea shelf. *Continental Shelf Research*, 5(1–2), 23–108. [https://doi.org/10.1016/0278-4343\(86\)90011-7](https://doi.org/10.1016/0278-4343(86)90011-7)
- Coyle, K. O., Eisner, L. B., Mueter, F. J., Pinchuk, A. I., Janout, M. A., Cieciel, K. D., ... Andrews, A. G. (2011). Climate change in the southeastern Bering Sea: Impacts on pollock stocks and implications for the oscillating control hypothesis. *Fisheries Oceanography*, 20(2), 139–156. <https://doi.org/10.1111/j.1365-2419.2011.00574.x>
- Currie, J. C., Thorson, J. T., Sink, K. J., Atkinson, L. J., Fairweather, T. P., & Winker, H. (2019). A novel approach to assess distribution trends from fisheries survey data. *Fisheries Research*, 214, 98–109. <https://doi.org/10.1016/j.fishres.2019.02.004>
- Danielson, S., Curchitser, E., Hedstrom, K., Weingartner, T., & Stabeno, P. (2011). On ocean and sea ice modes of variability in the Bering Sea. *Journal of Geophysical Research, Oceans*, 116(C12), C12034. <https://doi.org/10.1029/2011JC007389>
- De Robertis, A., & Cokelet, E. D. (2012). Distribution of fish and macrozooplankton in ice-covered and open-water areas of the eastern Bering Sea. *Deep Sea Research Part II: Topical Studies in Oceanography*, 65, 217–229. <https://doi.org/10.1016/j.dsr2.2012.02.005>
- Duffy-Anderson, J. T., Stabeno, P. J., Siddon, E. C., Andrews, A. G., Cooper, D. W., Eisner, L. B., Farley, E. V., Harpole, C. E., Heintz, R. A., Kimmel, D. G., Sewall, F. F., Spear, A. H., & Yasumishii, E. C. (2017). Return of warm conditions in the southeastern Bering Sea: Phytoplankton–fish. *PLoS ONE*, 12(6), e0178955. <https://doi.org/10.1371/journal.pone.0178955>
- Duffy-Anderson, J. T., Stabeno, P., Andrews, A. G. III, Cieciel, K., Deary, A., Farley, E., Fugate, C., Harpole, C., Heintz, R., Kimmel, D., Kuletz, K., Lamb, J., Paquin, M., Porter, S., Rogers, L., Spear, A., & Yasumiishi, E. (2019). Responses of the northern Bering Sea and southeastern Bering Sea pelagic ecosystems following record-breaking low winter sea ice. *Geophysical Research Letters*, 46(16), 9833–9842. <https://doi.org/10.1029/2019GL083396>
- Eisner, L. B., Zuenko, Y. I., Basyuk, E. O., Britt, L. L., Duffy-Anderson, J. T., Kotwicki, S., Ladd, C., & Cheng, W. (2020). Environmental impacts on walleye pollock (*Gadus chalcogrammus*) distribution across the Bering Sea shelf. *Deep Sea Research Part II: Topical Studies in Oceanography*, 181–182, 104881. <https://doi.org/10.1016/j.dsr2.2020.104881>
- Fournier, D. A., Skaug, H. J., Ancheta, J., Ianelli, J., Magnusson, A., Maunder, M. N., Nielsen, A., & Sibert, J. (2012). AD model builder: Using automatic differentiation for statistical inference of highly parameterized complex nonlinear models. *Optimization Methods and Software*, 27(2), 233–249. <https://doi.org/10.1080/10556788.2011.597854>

- Grimmer, M. (1963). The space-filtering of monthly surface temperature anomaly data in terms of pattern, using empirical orthogonal functions. *Quarterly Journal of the Royal Meteorological Society*, 89(381), 395–408. <https://doi.org/10.1002/qj.49708938111>
- Grüss, A., Thorson, J. T., Carroll, G., Ng, E. L., Holsman, K. K., Aydin, K., ... Thompson, K. A. (2020). Spatio-temporal analyses of marine predator diets from data-rich and data-limited systems. *Fish and Fisheries*, 21(4), 718–739. <https://doi.org/10.1111/faf.12457>
- Grüss, A., Thorson, J. T., Stawitz, C. C., Reum, J. C., Rohan, S. K., & Barnes, C. L. (2021). Synthesis of interannual variability in spatial demographic processes supports the strong influence of cold-pool extent on eastern Bering sea walleye pollock (*Gadus chalcogrammus*). *Progress in Oceanography*, 194, 102569. <https://doi.org/10.1016/j.pocan.2021.102569>
- Hartig, F. (2022). DHARMa: Residual diagnostics for hierarchical (multi-level/mixed) regression models. R package version 0.4.5. <https://CRAN.R-project.org/package=DHARMa>
- Hollowed, A. B., Barbeaux, S. J., Cokelet, E. D., Farley, E., Kotwicki, S., Ressler, P. H., Spital, C., & Wilson, C. D. (2012). Effects of climate variations on pelagic ocean habitats and their role in structuring forage fish distributions in the Bering Sea. *Deep Sea Research Part II: Topical Studies in Oceanography*, 65, 230–250. <https://doi.org/10.1016/j.dsr2.2012.02.008>
- Holsman, K. K., Ianelli, J., Aydin, K., Punt, A. E., & Moffitt, E. A. (2016). A comparison of fisheries biological reference points estimated from temperature-specific multi-species and single-species climate-enhanced stock assessment models. *Deep Sea Research Part II: Topical Studies in Oceanography*, 134, 360–378. <https://doi.org/10.1016/j.dsr2.2015.08.001>
- Hunt, G. L. Jr., Coyle, K. O., Eisner, L. B., Farley, E. V., Heintz, R. A., Mueter, F., Napp, J. M., Overland, J. E., Ressler, P. H., Salo, S., & Stabeno, P. J. (2011). Climate impacts on eastern Bering Sea food-webs: A synthesis of new data and an assessment of the oscillating control hypothesis. *ICES Journal of Marine Science*, 68(6), 1230–1243. <https://doi.org/10.1093/icesjms/fsr036>
- Ianelli, J. N., Barbeaux, S., Walters, G., & Williamson, N. (2003). Eastern Bering Sea walleye pollock stock assessment. In *Stock assessment and fishery evaluation report for the groundfish resources of the Bering Sea/Aleutian Islands regions* (p. 605). North Pacific Fishery Management Council.
- Karp, M. A., Peterson, J. O., Lynch, P. D., Griffis, R. B., Adams, C. F., Arnold, W. S., Barnett, L. A., deReynier, Y., DiCosimo, J., Fenske, K. H., & Gaichas, S. K. (2019). Accounting for shifting distributions and changing productivity in the development of scientific advice for fishery management. *ICES Journal of Marine Science*, 76(5), 1305–1315. <https://doi.org/10.1093/icesjms/fsz048>
- Kearney, K., Hermann, A., Cheng, W., Ortiz, I., & Aydin, K. (2020). A coupled pelagic–benthic–sympagic biogeochemical model for the Bering Sea: Documentation and validation of the BESTNPZ model (v2019.08.23) within a high-resolution regional ocean model. *Geoscientific Model Development*, 13(2), 597–650. <https://doi.org/10.5194/gmd-13-597-2020>
- Kidson, J. W. (1975). Tropical eigenvector analysis and the southern oscillation. *Monthly Weather Review*, 103(3), 187–196. [https://doi.org/10.1175/1520-0493\(1975\)103<0187:TEAATS>2.0.CO;2](https://doi.org/10.1175/1520-0493(1975)103<0187:TEAATS>2.0.CO;2)
- Kinder, T. H., & Schumacher, J. D. (1981). *Hydrographic structure. The eastern Bering Sea shelf: Oceanography and resources* (Vol. 1, p. 31).
- Kotwicki, S., & Lauth, R. R. (2013). Detecting temporal trends and environmentally-driven changes in the spatial distribution of bottom fishes and crabs on the eastern Bering Sea shelf. *Deep Sea Research Part II: Topical Studies in Oceanography*, 94, 231–243. <https://doi.org/10.1016/j.dsr2.2013.03.017>
- Kotwicki, S., Buckley, T. W., Honkalehto, T., & Walters, G. (2005). Variation in the distribution of walleye pollock (*Theragra chalcogramma*) with temperature and implications for seasonal migration. *Fishery Bulletin*, 103, 574–587.
- Kristensen, K., Bell, B., & Skaug, H. (2020). *Template model builder: A general random effect tool inspired by 'ADMB'*.
- Lauth, R. R., Dawson, E. J., & Conner, J. (2019). Results of the 2017 eastern and northern Bering Sea continental shelf bottom trawl survey of groundfish and invertebrate fauna. *National Marine Fisheries Service*, 1–265.
- Link, J. S., Nye, J. A., & Hare, J. A. (2011). Guidelines for incorporating fish distribution shifts into a fisheries management context. *Fish and Fisheries*, 12(4), 461–469. <https://doi.org/10.1111/j.1467-2979.2010.00398.x>
- Litzow, M. A. (2017). Indications of hysteresis and early warning signals of reduced community resilience during a Bering Sea cold anomaly. *Marine Ecology Progress Series*, 571, 13–28. <https://doi.org/10.3354/meps12137>
- Loughlin, T. R., & Miller, R. V. (1989). Growth of the northern fur seal colony on Bogoslof Island, Alaska. *Arctic*, 42, 368–372. <https://doi.org/10.14430/arctic1680>
- Mantua, N. J., Hare, S. R., Zhang, Y., Wallace, J. M., & Francis, R. C. (1997). A Pacific interdecadal climate oscillation with impacts on Salmon production. *Bulletin of the American Meteorological Society*, 78, 1069–1079. [https://doi.org/10.1175/1520-0477\(1997\)078<1069:APICOW>2.0.CO;2](https://doi.org/10.1175/1520-0477(1997)078<1069:APICOW>2.0.CO;2)
- Maureaud, A., Frelat, R., Pécuchet, L., Shackell, N., Mérigot, B., Pinsky, M. L., ... Thorson, J. T. (2021). Are we ready to track climate-driven shifts in marine species across international boundaries?—A global survey of scientific bottom trawl data. *Global Change Biology*, 27(2), 220–236.
- McGowan, J. A., Cayan, D. R., & Dorman, L. M. (1998). Climate-ocean variability and ecosystem response in the Northeast Pacific. *Science*, 281(5374), 210–217. <https://doi.org/10.1126/science.281.5374.210>
- Moriarty, M., Sethi, S. A., Pedreschi, D., Smeltz, T. S., McGonigle, C., Harris, B. P., Wolf, N., & Greenstreet, S. P. R. (2020). Combining fisheries surveys to inform marine species distribution modeling. *ICES Journal of Marine Science*, 77, 539–552. <https://doi.org/10.1093/icesjms/fsz254>
- Mueter, F. J., & Litzow, M. A. (2008). Sea ice retreat alters the biogeography of the Bering Sea continental shelf. *Ecological Applications*, 18(2), 309–320. <https://doi.org/10.1890/07-0564.1>
- Mueter, F. J., Ladd, C., Palmer, M. C., & Norcross, B. L. (2006). Bottom-up and top-down controls of walleye pollock (*Theragra chalcogramma*) on the Eastern Bering Sea shelf. *Progress in Oceanography*, 68(2–4), 152–183. <https://doi.org/10.1016/j.pocan.2006.02.012>
- Nichol, D. G., Kotwicki, S., Wilderbuer, T. K., Lauth, R. R., & Ianelli, J. N. (2019). Availability of yellowfin sole *Limanda aspera* to the eastern Bering Sea trawl survey and its effect on estimates of survey biomass. *Fisheries Research*, 211, 319–330. <https://doi.org/10.1016/j.fishres.2018.11.017>
- Nye, J. A., Link, J. S., Hare, J. A., & Overholtz, W. J. (2009). Changing spatial distribution of fish stocks in relation to climate and population size on the Northeast United States continental shelf. *Marine Ecology Progress Series*, 393, 111–129. <https://doi.org/10.3354/meps08220>
- O'Leary, C. A., DeFilippo, L. B., Thorson, J. T., Kotwicki, S., Hoff, G. R., Kulik, V. V., Ianelli, J. N., & Punt, A. E. (2022). Understanding transboundary stocks' availability by combining multiple fisheries-independent surveys and oceanographic conditions in spatiotemporal models. *ICES Journal of Marine Science*, 79(4), 1063–1074.
- O'Leary, C. A., Kotwicki, S., Hoff, G. R., Thorson, J. T., Kulik, V. V., Ianelli, J. N., Lauth, R. R., Nichol, D. G., Conner, J., & Punt, A. E. (2021). Estimating spatiotemporal availability of transboundary fishes to fishery-independent surveys. *Journal of Applied Ecology*, 58(10), 2146–2157. <https://doi.org/10.1111/1365-2664.13914>
- O'Leary, C. A., Thorson, J. T., Ianelli, J. N., & Kotwicki, S. (2020). Adapting to climate-driven distribution shifts using model-based indices and age



- composition from multiple surveys in the walleye pollock (*Gadus chalcogrammus*) stock assessment. *Fisheries Oceanography*, 29(6), 541–557. <https://doi.org/10.1111/fog.12494>
- Perry, A. L., Low, P. J., Ellis, J. R., & Reynolds, J. D. (2005). Climate change and distribution shifts in marine fishes. *Science*, 308(5730), 1912–1915. <https://doi.org/10.1126/science.1111322>
- Pinsky, M. L., Reygondeau, G., Caddell, R., Palacios-Abrantes, J., Spijkers, J., & Cheung, W. W. (2018). Preparing ocean governance for species on the move. *Science*, 360(6394), 1189–1191. <https://doi.org/10.1126/science.aat2360>
- Pinsky, M. L., Worm, B., Fogarty, M. J., Sarmiento, J. L., & Levin, S. A. (2013). Marine taxa track local climate velocities. *Science*, 341(6151), 1239–1242. <https://doi.org/10.1126/science.1239352>
- R Core Team. R Foundation for Statistical Computing. (2015). *R: A language and environment for statistical computing*. Austria. <http://www.R-project.org>
- Siddon, E. (2022). *Ecosystem status report 2022: Eastern Bering Sea, stock assessment and fishery evaluation report, North Pacific Fishery Management Council, 1007 West 3rd Ave., Suite 400, Anchorage, Alaska 99501*.
- Sigler, M. F., Napp, J. M., Stabeno, P. J., Heintz, R. A., Lomas, M. W., & Hunt, G. L. Jr. (2016). Variation in annual production of copepods, euphausiids, and juvenile walleye pollock in the southeastern Bering Sea. *Deep Sea Research Part II: Topical Studies in Oceanography*, 134, 223–234. <https://doi.org/10.1016/j.dsr2.2016.01.003>
- Skaug, H. J., & Fournier, D. A. (2006). Automatic approximation of the marginal likelihood in non-Gaussian hierarchical models. *Computational Statistics & Data Analysis*, 51(2), 699–709. <https://doi.org/10.1016/j.csda.2006.03.005>
- Smith, J. A., Buil, M. P., Muhling, B., Tommasi, D., Brodie, S., Frawley, T. H., ... Jacox, M. G. (2023). Projecting climate change impacts from physics to fisheries: A view from three California current fisheries. *Progress in Oceanography*, 211, 102973. <https://doi.org/10.1016/j.pocean.2023.102973>
- Smith, J. Q. (1985). Diagnostic checks of non-standard time series models. *Journal of Forecasting*, 4(3), 283–291. <https://doi.org/10.1002/for.3980040305>
- Spies, I., Gruenthal, K. M., Drinan, D. P., Hollowed, A. B., Stevenson, D. E., Tarpey, C. M., & Hauser, L. (2020). Genetic evidence of a northward range expansion in the eastern Bering Sea stock of Pacific cod. *Evolutionary Applications*, 13(2), 362–375. <https://doi.org/10.1111/eva.12874>
- Stabeno, P. J., & Bell, S. W. (2019). Extreme conditions in the Bering Sea (2017–2018): Record-breaking low sea-ice extent. *Geophysical Research Letters*, 46(15), 8952–8959. <https://doi.org/10.1029/2019GL083816>
- Stabeno, P. J., Bond, N. A., & Salo, S. A. (2007). On the recent warming of the southeastern Bering Sea shelf. *Deep Sea Research Part II: Topical Studies in Oceanography*, 54(23–26), 2599–2618. <https://doi.org/10.1016/j.dsr2.2007.08.023>
- Stabeno, P. J., Bond, N. A., Kachel, N. B., Salo, S. A., & Schumacher, J. D. (2001). On the temporal variability of the physical environment over the south-eastern Bering Sea. *Fisheries Oceanography*, 10(1), 81–98. <https://doi.org/10.1046/j.1365-2419.2001.00157.x>
- Stabeno, P. J., Kachel, N. B., Moore, S. E., Napp, J. M., Sigler, M., Yamaguchi, A., & Zerbini, A. N. (2012). Comparison of warm and cold years on the southeastern Bering Sea shelf and some implications for the ecosystem. *Deep Sea Research Part II: Topical Studies in Oceanography*, 65, 31–45. <https://doi.org/10.1016/j.dsr2.2012.02.020>
- Stabeno, P. J., Kachel, N. B., Sullivan, M., & Whitley, T. E. (2002). Variability of physical and chemical characteristics along the 70-m isobath of the southeastern Bering Sea. *Deep Sea Research Part II: Topical Studies in Oceanography*, 49(26), 5931–5943. [https://doi.org/10.1016/S0967-0645\(02\)00327-2](https://doi.org/10.1016/S0967-0645(02)00327-2)
- Stabeno, P., Napp, J., Mordy, C., & Whitley, T. (2010). Factors influencing physical structure and lower trophic levels of the eastern Bering Sea shelf in 2005: Sea ice, tides and winds. *Progress in Oceanography*, 85(3–4), 180–196. <https://doi.org/10.1016/j.pocean.2010.02.010>
- Stepanenko, M. A., & Gritsay, E. V. (2016). Assessment of stock, spatial distribution, and recruitment of walleye pollock in the northern and eastern Bering Sea. *Известия ТИНРО*, 185, 16–30. <https://doi.org/10.26428/1606-9919-2016-185-16-30>
- Stevenson, D. E., & Lauth, R. R. (2019). Bottom trawl surveys in the northern Bering Sea indicate recent shifts in the distribution of marine species. *Polar Biology*, 42(2), 407–421. <https://doi.org/10.1007/s00300-018-2431-1>
- Thorson, J. T. (2018). Three problems with the conventional delta-model for biomass sampling data, and a computationally efficient alternative. *Canadian Journal of Fisheries and Aquatic Sciences*, 75(9). <https://doi.org/10.1139/cjfas-2017-0266>
- Thorson, J. T. (2019). Measuring the impact of oceanographic indices on species distribution shifts: The spatially varying effect of cold-pool extent in the eastern Bering Sea. *Limnology and Oceanography*, 64(6), 2632–2645. <https://doi.org/10.1002/lno.11238>
- Thorson, J. T., & Barnett, L. A. (2017). Comparing estimates of abundance trends and distribution shifts using single- and multispecies models of fishes and biogenic habitat. *ICES Journal of Marine Science*, 74(5), 1311–1321. <https://doi.org/10.1093/icesjms/fsw193>
- Thorson, J. T., & Kristensen, K. (2016). Implementing a generic method for bias correction in statistical models using random effects, with spatial and population dynamics examples. *Fisheries Research*, 175, 66–74. <https://doi.org/10.1016/j.fishres.2015.11.016>
- Thorson, J. T., Arimitsu, M. L., Barnett, L. A., Cheng, W., Eisner, L. B., Haynie, A. C., Hermann, A. J., Holsman, K., Kimmel, D. G., Lomas, M. W., Richar, J., & Siddon, E. C. (2021). Forecasting community reassembly using climate-linked spatio-temporal ecosystem models. *Ecography*, 44(4), 612–625. <https://doi.org/10.1111/ecog.05471>
- Thorson, J. T., Cheng, W., Hermann, A. J., Ianelli, J. N., Litzow, M. A., O'Leary, C. A., & Thompson, G. G. (2020). Empirical orthogonal function regression: Linking population biology to spatially varying environmental conditions using climate projections. *Global Change Biology*, 26(8), 4638–4649. <https://doi.org/10.1111/gcb.15149>
- Thorson, J. T., Ciannelli, L., & Litzow, M. A. (2020). Defining indices of ecosystem variability using biological samples of fish communities: A generalization of empirical orthogonal functions. *Progress in Oceanography*, 181, 102244. <https://doi.org/10.1016/j.pocean.2019.102244>
- Thorson, J. T., Ianelli, J. N., Larsen, E. A., Ries, L., Scheuerell, M. D., Szuwalski, C., & Zipkin, E. F. (2016). Joint dynamic species distribution models: A tool for community ordination and spatio-temporal monitoring. *Global Ecology and Biogeography*, 25(9), 1144–1158. <https://doi.org/10.1111/geb.12464>
- Thorson, J. T., Pinsky, M. L., & Ward, E. J. (2016). Model-based inference for estimating shifts in species distribution, area occupied and centre of gravity. *Methods in Ecology and Evolution*, 7(8), 990–1002. <https://doi.org/10.1111/2041-210X.12567>
- Thorson, J. T., Shelton, A. O., Ward, E. J., & Skaug, H. J. (2015). Geostatistical delta-generalized linear mixed models improve precision for estimated abundance indices for West Coast groundfishes. *ICES Journal of Marine Science*, 72(5), 1297–1310. <https://doi.org/10.1093/icesjms/fsu243>
- Vestfals, C. D., Ciannelli, L., & Hoff, G. R. (2016). Changes in habitat utilization of slope-spawning flatfish across a bathymetric gradient. *ICES Journal of Marine Science*, 73(7), 1875–1889. <https://doi.org/10.1093/icesjms/fsw112>

- Volvenko, I. V., Orlov, A. M., Gebruk, A. V., Katugin, O. N., Vinogradov, G. M., & Maznikova, O. A. (2018). Species richness and taxonomic composition of trawl macrofauna of the North Pacific and its adjacent seas. *Scientific Reports*, 8(1), 16604. <https://doi.org/10.1038/s41598-018-34819-4>
- Warton, D. I., Thibaut, L., & Wang, Y. A. (2017). The PIT-trap—A “model-free” bootstrap procedure for inference about regression models with discrete, multivariate responses. *PLoS ONE*, 12(7), e0181790. <https://doi.org/10.1371/journal.pone.0181790>
- Wyllie-Echeverria, T. I. N. A., & Wooster, W. S. (1998). Year-to-year variations in Bering Sea ice cover and some consequences for fish distributions. *Fisheries Oceanography*, 7(2), 159–170. <https://doi.org/10.1046/j.1365-2419.1998.00058.x>
- Zador, S., Aydin, K., & Cope, J. (2011). Fine-scale analysis of arrowtooth flounder *Atheresthes stomias* catch rates reveals spatial trends in abundance. *Marine Ecology Progress Series*, 438, 229–239. <https://doi.org/10.3354/meps09316>

## SUPPORTING INFORMATION

Additional supporting information can be found online in the Supporting Information section at the end of this article.

**How to cite this article:** DeFilippo, L. B., Thorson, J. T., O'Leary, C. A., Kotwicki, S., Hoff, J., Ianelli, J. N., Kulik, V. V., & Punt, A. E. (2023). Characterizing dominant patterns of spatiotemporal variation for a transboundary groundfish assemblage. *Fisheries Oceanography*, 1–18. <https://doi.org/10.1111/fog.12651>